Characterizing Microbial Denitrification and Biogeochemical Processes Within and Surrounding a NITREX™ Permeable Reactive Barrier in Waquoit Bay, MA

A senior thesis submitted to the Department of Biology, Colorado College

By: Collin Knauss

Department of Biology, Colorado College, Colorado Springs, CO

Bachelor of Arts Degree in Biology
May 2013

Approved by:

Primary Thesis Advisor: Dr. Mark Wilson

Secondary Thesis Advisor: Dr. Miroslav Kummel

Table of Contents

Abstract:

Aquatic ecosystems around the globe face an increasing threat of eutrophication from algal blooms caused by excess nutrients. On Cape Cod, the major route for delivery of the limiting nutrient, nitrogen, to coastal ponds and estuaries is groundwater seepage. In 2005, researchers at the Woods Hole Marine Biological Laboratory installed and began monitoring a wood-chip based NITREX^{TM} permeable reactive barrier (PRB) designed to remove nitrates via denitrification at the shore of Waquoit Bay, MA. In this experiment, I took groundwater samples from an array of multi-depth sampling wells within and surrounding the PRB. From each well I measured a suite of physico-chemical parameters and in a subset of samples I analyzed metagenomic DNA for the presence and abundance of the *nirS* nitrite reductase gene and examined the structure of the microbial community using denaturing gradient gel electrophoresis (DGGE) of the 16S rRNA gene. The PRB effectively reduced the nitrates from a maximum concentration of 109 μM in the core of the nutrient plume to below 10 μM inside and down-gradient of the PRB; however, a portion of the nitrate plume persisted at 3 meter depths underneath the PRB. Hydrogen sulfides present inside the PRB suggest seawater intrusion stimulates sulfate-reducing bacteria that may compete with denitrifiers for resources. Dissolved inorganic carbon (DIC) from respiration increased from 780 μM in the up-gradient groundwater to a maximum of 1985 μM inside the PRB. Dissolved organic carbon (DOC) increased from 8 μM in the inflowing up-gradient groundwater to a maximum of 130 μM in the PRB. High DOC concentrations extended down-gradient beyond the PRB. The presence and abundance of the *nir*S nitrite reductase gene, determined by PCR and qPCR, also increased inside and down-gradient of the PRB. DGGE results indicate the presence of distinct microbial communities among the sites. There was a high similarity between up-gradient PRB samples and control samples, with a different community emerging within the PRB, indicating that the PRB does have a measurable effect on microbial community composition.

Introduction:

Nitrate (NO_3) concentrations in groundwater and rivers around the globe have increased substantially due to synthetic nitrogen fertilizers and wastewater input, and as a result there has been heightened interest in biological NO_3 removal (Burgin and Hamilton, 2007). Biological removal of NO_3 from contaminated groundwater entering estuaries usually occurs from assimilation into microbial or algal biomass, or from dissimilatory denitrification by bacteria. In ecosystems with high nitrogen inputs, denitrification provides nitrogen load reduction thereby contributing to eutrophication control (Nogales et al., 2002). Dissimilatory denitrification is an anaerobic process in which microbes use oxidized nitrogen compounds (e.g. NO_3) as a terminal electron acceptor to break down organic matter and generate energy for metabolic processes (Braker et al., 1998). This process can be seen by the following equation:

$$\mathbf{4NO_3^- + 4H^+ + 5CH_2O \rightarrow 5CO_2 + 2N_2 + 7H_2O}$$

Waquoit Bay in Falmouth, MA, USA, like many other estuaries around the globe, has experienced significant anthropogenic nitrogen loading, with a twofold increase in total nitrogen inputs between 1938 and 1990 (Bowen and Valiela, 2001; Howarth et al., 2000). As a result of the increased nitrogen input into the Bay, nitrogen-induced eutrophication is now a serious threat to the Bay's health (Serveiss et al., 2004). Remediation of excess nitrogen loading can be achieved through various means including construction of centralized sewage treatment facilities, wide-scale implementation of on-site denitrifying septic systems or composting toilets, and a reduction in residential application of fertilizers to lawns and agriculture. However, these approaches are costly, may take a long time to implement and may not be widely embraced by individual

homeowners. Installation of a porous reactive barrier along the shore to intercept and remove NO_3 in groundwater by increasing denitrification is an innovative alternative approach to reduce nitrogen loading that might prove cost effective (Robertson et al., 2005a and b).

In 2005, Drs. Kenneth Foreman and Joseph Vallino from the Marine Biological Laboratory in Woods Hole MA, and Pio Lombardo of Lombardo Associates in Newton, MA built and began testing two permeable reactive barriers (PRBs) composed of wood chips mixed with limestone (NITREX^{TM}) along the shores of Waquoit Bay and Childs River. Most denitrifying bacteria depend on external organic carbon sources to stimulate denitrification rates. The PRBs aim to capture and remove NO_3-rich groundwater by providing a slowly decomposing carbon source to stimulate denitrifying bacteria and fuel NO_3 removal under anaerobic conditions (Robertson et al., 2005; Schipper et al., 2010).

Denitrifying bacteria are phylogenetically diverse, belonging to most major physiological groups (Braker et al., 1998). Classified as facultative anaerobes, denitrifying bacteria can switch from oxygen to nitrogen oxides as terminal electron acceptors under anoxic conditions (Braker et al., 1998). Nitrite reductase, a key enzyme in the dissimilatory denitrification process, can be generated by two separate nitrite reductase genes: one contains copper encoded by the *nir*K gene, the other contains heme c and heme d_1 (cytochrome cd_1) encoded by the *nir*S gene (Braker et al., 1998). While both enzymes are structurally different, their functional equivalence in catalyzing nitrite reduction makes these genes useful targets for identifying denitrifying bacterial communities (Figure 1) (Braker et al., 2000). For the purposes of this experiment, I only

tested for *nir*S gene expression because it is more widely distributed in marine systems than *nir*K in denitrifying bacteria (Braker et al., 1998).

Figure 1. The process of denitrification with chemical transformations of NO_3 to N_2 and the associated enzymes during intermediate steps (Jones, 2010).

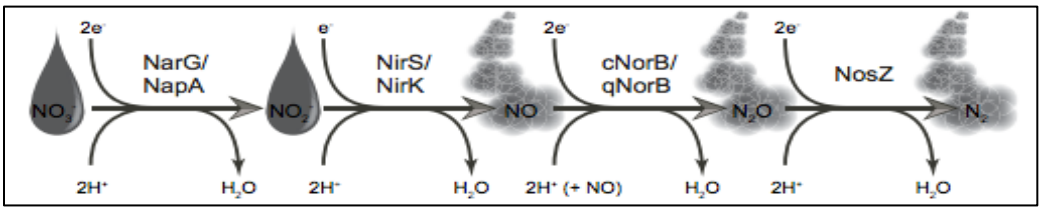

While the success in promoting denitrification has been confirmed at both PRBs (Vincent, 2006), several questions remain before large-scale implementation on the shores of Waquoit Bay should be implemented. For example, seawater intrusion into the Waquoit Bay PRB has become a rising concern for the effectiveness of denitrification. First, seawater inundation on top of the PRB may displace the groundwater, forcing NO_3 beneath the PRB. Additionally, the introduction of seawater into the PRB has been shown to stimulate sulfate (SO_4) reduction (Vincent, 2006), which may compete with NO_3 reduction. Also, hydrogen sulfides (H_2S) produced during SO_4 reduction may lead NO_3 to undergo dissimilatory NO_3 reduction to ammonium (NH_4) (DNRA) rather than denitrification, because free sulfides have been shown to inhibit the final two reduction steps of denitrification (Burgin and Hamilton, 2007; Brunet and Garcia-Gil, 1996). However, in the presence of reduced sulfur in the form of elemental sulfur or metal-bound sulfides (FeS), the system favors denitrification (NO_3 directly transformed to N_2 gas) (Figure 2) (Burgin and Hamilton, 2007).

Figure 2. A simplified diagram showing the different potential NO_3 removal pathways. (Burgin and Hamilton, 2007).

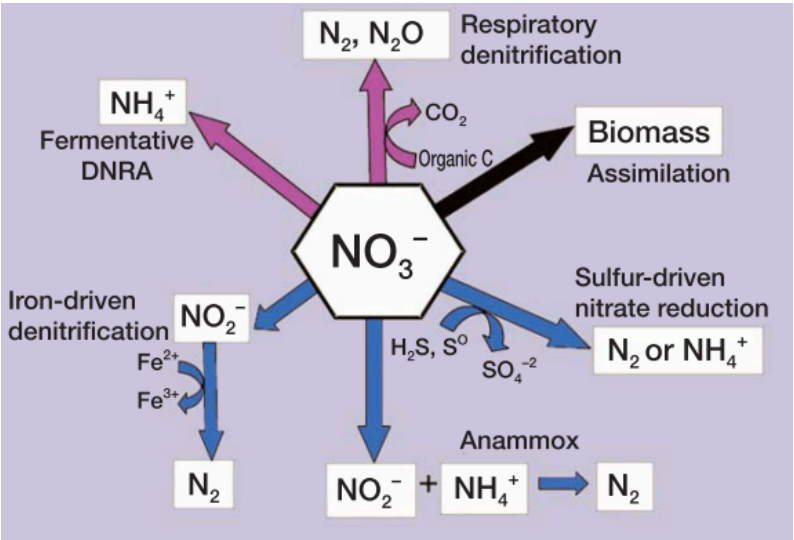

My goal was to characterize the biogeochemical and denitrifying dynamics occurring in the PRB vicinity by looking at dissolved organic carbon (DOC), dissolved inorganic carbon (DIC), NO_3, NH_4, SO_4 and H_2S. Specifically, I wanted to see if the presence of the PRB significantly changed the concentration of these various parameters from up-gradient locations to within PRB and down-gradient locations. I predicted that increased abundance of the *nir*S gene would co-occur with increased concentrations of DOC provided by the PRB. I also hypothesized that there would be a greater potential for further denitrification down-gradient as a result of increased carbon being pulled out of the PRB, thereby expanding the effectiveness of the PRB. Further, I expected the PRB site would have higher microbial community composition and distinct microbial groups from an adjacent control site as a result of the altered biogeochemistry. I also hypothesized that the microbial diversity up-gradient of the PRB would have a higher similarity to the control samples than to the PRB samples.

Methods:

Site description:

The PRB sampled in this study is located at the head of Waquoit Bay in Falmouth, MA, USA (Figure 3). The PRB is located above the mean high tide line about 0.5-1 meters below grade and below the top of the water table. It is approximately 3.5 meters wide, 2 meters deep and 20 meters long filled with limestone buffered woodchip media (Robertson et al., 2005a). I sampled during the fall of 2011 on 11/18/11 and returned to sample during the summer of 2012 on 6/7/12.

Figure 3. Map of Waquoit Bay, MA, USA with the location of the NITREX^{TM} Permeable Reactive Barrier marked by the yellow star.

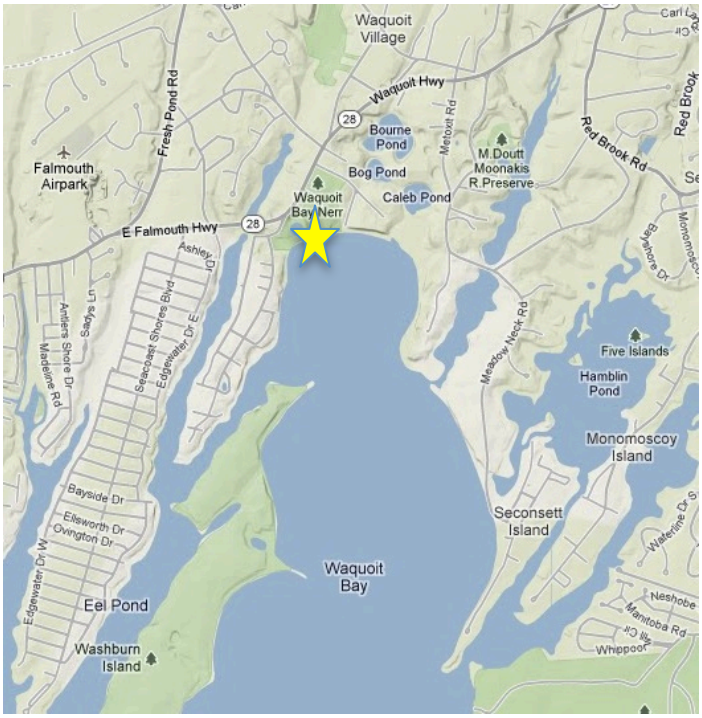

Sample Collection:

During the initial fall 2011 sampling period, a peristaltic pump was used to collect groundwater from multi-depth sampling wells located around the PRB (Figure 4). Groundwater was collected from 32 sites for nutrient analysis, 12 of which were also sampled for *nir*S genetic analysis of the bacterial community. Water for the extraction of DNA was collected into 1 L Nalgene polycarbonate bottles. The 12 one-liter Nalgene bottles containing the DNA samples were filtered in the lab using 0.22 micron Sterivex™ filters. Using a pre-designed setup with the male end of the Sterivex™ filter attached to the top of the female adapter and an autoclaved syringe attached to the top of the Sterivex™ filter, samples were poured into the syringe and the pump was turned on after opening the t-valves. After pumping the samples through, the t-valves were closed and the Sterivex™ filters were removed and stored in a -80 °C freezer. Prior to filling sample bottles, groundwater was pumped past a Quanta Hydrolab sensor array to measure salinity, pH, temperature, conductivity, and DO. Once temperature and DO values stabilized, samples were collected for SO_4/chlorides (Cl^-), H_2S, NO_3, NH_4, DIC and DOC.

NH_4 and NO_3 samples were filtered into acid-washed 20 ml plastic scintillation vials in the field using a Swinnex® filter holder with Whatman™ 0.25 mm GFF filters and then put on ice. In the lab, NH_4 samples were acidified with 20 µl of 5 N HCl (1 µl of HCl per ml of sample) and then stored at 4 °C in the fridge until later analysis. NO_3 samples were bubbled with hydrated N_2 gas to remove H_2S and then frozen until later analysis.

SO_4/Cl^-, H_2S and DIC samples were collected into 60 ml biological oxygen demand (BOD) bottles. The bottles were flushed with three 60 ml volumes of sample water

during collection capping to avoid trapping air bubbles. In the lab, 250 µl of sample was pipetted from the 60 ml BOD bottle into non-acid washed vials that were prefilled with 6 ml of 2% zinc acetate for H_2S analysis. A 5 ml sample was drawn using a 20 ml syringe for DIC analysis. Approximately 10 ml of sample was transferred from the 60 ml BOD bottle into acid-washed plastic scintillation vials for SO_4/Cl^- analysis and then bubbled with hydrated N_2 gas to remove H_2S that might oxidize back to SO_4, thereby altering the ratio. The SO_4/Cl^- samples were refrigerated until later analysis. DOC samples were filtered (25 mm acid rinsed GFF) into 30 ml acid-washed glass scintillation vials with Teflon lined caps to prevent carbon contamination and then acidified with 50 µl of 85% phosphoric acid to remove DIC.

On returning to the PRB site during the summer of 2012, I constructed adjacent control sampling sites. Groundwater was collected from 27 PRB sites and 17 control sites for nutrient analyses and microbial community DNA analysis. I evaluated total microbial diversity of the PRB and control sites through targeting the 16S rRNA universal bacteria gene. Groundwater was filtered directly onto 0.22 micron Sterivex™ filters in the field to collect microbial DNA and the filters were immediately frozen in liquid nitrogen. Prior to filling sample bottles, groundwater was pumped past a Quanta Hydrolab sensor array to measure salinity, pH, temperature, conductivity, and DO.

Figure 4. Cross-section of NITREX™ Permeable Reactive Barrier in Waquoit Bay. Green line indicates relative elevation and gradient of beach slope towards Waquoit Bay (to the right of the image). Brown box describes the location of the PRB and the black dots represent sampling wells.

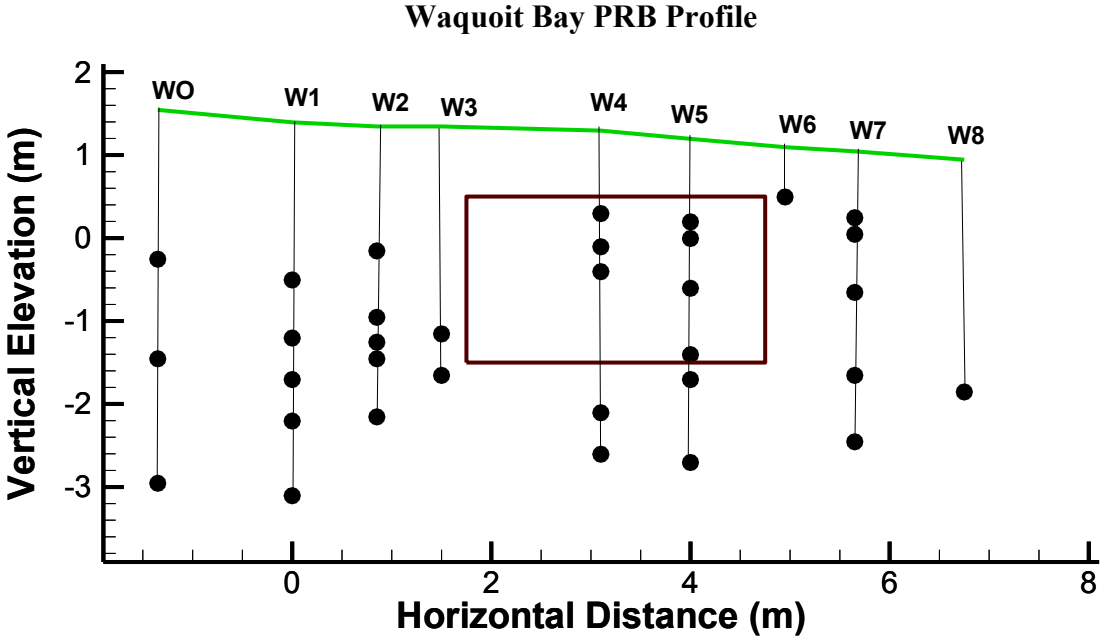

Analytical procedures:

DIC was immediately analyzed upon returning to lab. The 20 ml syringes containing five ml of sample were filled with 15 ml of air that was passed through a Drierite filled CO_2 trap. Two ml of sulfuric acid was injected into each 20 ml syringe, which was then shaken for two minutes. After equilibration, the headspace was then injected into a Shimadzu Gas Chromatograph GC-14A equipped with Thermal Conductivity Detector for measurement of CO_2.

NH_4 samples were analyzed using a method modified from Solarzano (1969). NO_3 samples were removed from the freezer the day of the analysis and allowed to thaw and then analyzed using a Lachat flow injection analyzer (FIA) (Loveland, CO) adapted from Wood et al. (1967). H_2S samples were analyzed using a method adapted from

Gilboa-Garber (1971). DOC samples were run on an Aurora 1030W TOC Analyzer (College Station, TX).

SO_4/Cl^- samples were diluted according to their salinity values: samples less than 0.10 ppt used a 1:1 dilution, samples less than 1.0 but greater than 0.10 ppt used a 50:1 and a 1:1 dilution, samples greater than 1.0 but less than 3.0 ppt used a 50:1 dilution and samples greater than 4.0 ppt used a 100:1 dilution. The samples were then loaded on a Dionex™ AS40 Automated Sampler and analyzed on a DX-120 Ion Chromatograph (Sunnyvale, CA).

DIC Resulting from Respiration:

Expected DIC was calculated using a standard mixing equation with Cl^- as a conservative tracer of the DIC species present in solution. Subtracting the expected DIC from the measured DIC produced DIC values resulting from respiration in the system. Cl^- was normalized to a 0→1 scale and Cl_{GW} and DIC_{GW} were obtained by averaging the Cl^- and DIC values for up-gradient wells that demonstrated no evidence of seawater intrusion. DIC_{SW} was obtained by averaging the sampling wells that demonstrated evidence of seawater intrusion.

X_{cl}=Normalized chloride values
Cl_{GW}=Chloride in groundwater
$Cl_{SW=}$Chloride in full strength seawater
Cl_M=Measured chloride
DIC_{GW}=DIC in groundwater
DIC_{SW}=DIC in seawater
DIC_E=Expected DIC
DIC_M=Measured DIC
ΔDIC=Change in DIC or respired DIC

$$X_{cl}=(Cl_M-Cl_{GW})/(Cl_{SW}-Cl_{GW})$$
$$DIC_E=DIC_{SW}+(1-X_{cl})(-DIC_{SW}+DIC_{GW})$$
$$\Delta DIC=DIC_M-DIC_E$$

Molecular Methods:

DNA Extraction:

DNA was extracted using a MOBIO PowerWater® Sterivex™ DNA Isolation Kit (Carlsbad, CA). To determine the presence of DNA, samples were analyzed by gel electrophoresis on 1% agarose gels followed by 15 min of staining with 1.75 µl of ethidium bromide and then run at 110 V for 30 min. Additionally, one µl of DNA from each sample was analyzed on a micro-volume UV-Vis NanoDrop 2000 Spectrophotometer for DNA concentration in ng per µl (Waltham, MA).

NirS PCR and qPCR:

After confirming the presence of DNA in each sample, DNA extractions were analyzed for the presence or absence of the *nir*S gene using PCR analysis on an Eppendorf Mastercycler®. The master mix per 25 µl reaction: 13.4 µl MilliQ water, 5 µl 5X PCR buffer, 0.5 µl of 10 mM dNTPs, 2.5 µl of 10 µM nirS1F primer (5'-CCTA(C/T)TGGCCGCC(A/G)CA(A/G)T-3'), 2.5 µl of 10 µM nirS6R primer (5'-CGTTGAACTT(A/G)CCGGT-3'), 0.1 µl of 5 units/µl Taq and 1 µl of template DNA (Braker et al. 1998). Samples were run using gel electrophoresis with 1% agarose and 1.75 µl of ethidium bromide at 110 V for 30 min to visualize the PCR product. Along with 24 µl of master mix solution, 1 µl of DNA from known denitrifiers was used as a positive control and 1 µl MilliQ water was used as a negative control. The cycles began with a denaturing step of 3 min at 94 °C followed by: 40 cycles of 40 sec at 94 °C, 40 sec at 56°C, and 1 min at 72°C. The cycles finished with 10 min of 72°C and an indefinite hold at 4°C.

Total abundance of the *nir*S gene in each of the samples was quantified using

quantitative PCR (qPCR). Samples and standards were run in triplicate on a Stratagene Mx3005P (Santa Clara, CA) following the method of Jayakumar et al. (2009). The reagents per 25 ul sample included 10 µl SYBR^{R} Green Q-PCR master mix, 3 µl of 10 µM nirS1F (5'-CCTA(C/T)TGGCCGCC(A/G)CA(A/G)T-3'), 3 µl of 10 µM nirS3R (5'-GCCGCCGTC(A/G)TG(A/C/G)AGGAA-3'), 0.3 µl reference dye (ROX), 1 µl DNA and 7.7 µl MilliQ water (Braker et al. 1998). In addition, two controls were run: a non-primer control with 24 µl of master mix solution without primers and 1 µl of PRB sample DNA and a non-DNA control with 25 µl of master mix solution. Samples were amplified using the following conditions: 95 °C for 15 min, followed by 40 cycles of 94 °C for 15 sec, 62 °C for 30 sec, and 72 °C for 30 sec. A stock solution with 7.46 X 10^{10} copy numbers of *nir*S was used to make standards in a seven-fold dilution series of 7.46 X 10^{8}→7.46 X 10^{3} copy numbers of nirS. The actual copy number per µl of DNA solution was calculated by converting the Ct (threshold cycle) value for each sample using the standard curve equation. To calculate copy number per ng of DNA, the copy number was divided by the NanoDrop DNA value obtained earlier in the experiment. Specificity of the qPCR reaction was assessed by examination of dissociation curves for all samples and standards.

16S rRNA PCR and DGGE:

After determining the amount of DNA in the Waquoit Bay samples, in ng/µl of DNA solution, I amplified the universal bacteria 16S rRNA gene using PCR analysis on a S1000 Thermal Cycler. A denaturing gradient gel electrophoresis of the 16S PCR product was run to determine potential variations in microbial genetic community composition in the Waquoit Bay PRB and control sites. PCR amplifications of the extracted DNA were

run after a series of optimization reactions for best reaction conditions. Samples were optimized using the following conditions per reaction: 11.2 µl of MilliQ water, 5 µl of 5X Taq buffer solution, 0.25 µl of 40 uM dNTPs, 2.5 µl of the 357gcF primer (5′-CGCCCGCCGCGCCCCGCGCCCGGCCCGCCGCCCCCGCCCCCCTACGGGAGGCAGCAG-3′), 2.5 µl of the 519r primer (5′-ACCGCGGCTGCTGGCAC-3′),1 µl of $MgCl_2$, 0.5 µl of Taq polymerase and 2.5 µl of template DNA (Bowen et al., 2009). A 25 ml gradient gel was prepared with 40% and 60% denaturants. The 40% gradient was made using: 7.5 ml of 0% denaturant, 5 ml of 100% denaturant, 10 µl of BPB (blue dye), 54.2 µl of APS and 4.375 µl of TEMED. The 60% gradient was prepared with 5 ml of 0% denaturant, 7.5 ml of 100% denaturant, 54.2 µl of APS and 4.375 µl of TEMED. A 0% stacking gel was prepared with 5 ml of 0% denaturant, 50 µl of APS and 5 µl of TEMED. A running buffer with 6,860 ml DI water and 140 ml of 50X TAE solution was poured into the gel holder apparatus. The samples were prepared with 4 µl of 2X loading dye and 15 µl of sample and then pipetted into wells. Gels were run at 60 °C for 17 hours at 100 V. After 17 hours, the gel was taken out and stained in a solution with 15 µl 10,000X SYBR gold and 150 ml new 50X TAE buffer (modified from Crump et al., 2004).

Statistical Analyses:

I performed paired t-tests using Microsoft Excel with several variables (DO, DOC, H_2S, DIC from respiration and *nir*S abundance) to statistically measure the PRB's influence on variable concentration from up-gradient regions to PRB/down-gradient regions. After finding the mean and standard deviation for each variable in the different

regions, I performed independent paired t-tests to see if the PRB had a significant effect. Additionally, I tested for causality between different variables. I looked for statistically significant linear regressions between independent variables (DO) and dependent variables (DOC, H_2S, DIC from respiration and nirS abundance). To do this, I needed to meet the assumptions of the linear regression analysis. Alternatively, I examined correlation by testing for the significance of the correlation coefficient between different variables. To do this I needed to find the appropriate t-value so I could test for significance of the correlation coefficient, r. I used the standard t distribution formula for causality and correlation tests:

$$\mathbf{t = r*SqRt[(n-2)/(1-r^2)]}$$

Data Processing and Contouring:

Results from nutrient and qPCR analyses were plotted either using Tecplot Focus software (Bellevue, WA) or using the RStudio application of R. In both cases, contours were drawn based on triangular interpolation. The beach gradient and vertical location of each sampling depth relative to sea level was determined using pre-existing survey data and measured from a permanent reference point (top of a gray pipe set into the beach) located 1.89 m above sea level. DGGE images were analyzed using Kodak molecular imaging software to identify banding patterns. The presence and absence of bands were transformed into a similarity matrix using the bray curtis similarity metric using Primer 5 (Plymouth Marine Laboratory) software. The similarities were visualized using multidimensional scaling (MDS) plots and cluster analyses.

Results:

DO 11/18/11:

DO was higher up-gradient of the PRB with wells 0, 1 and 2 showing the highest concentrations of around 7-8 mg/L in the upper sampling depths about 1-2 meters directly up-gradient of the PRB (Figure 5). Conditions inside the PRB were mostly anoxic with wells 4 and 5 showing DO of less than 1 mg/L for virtually all sampling depths. There was an isolated increase in DO around the bottom right side of the PRB with lower well 5 and 7 depths showing higher than expected DO values; however some of these wells showed bubble intrusion from possibly cracked plastic well tubing during my sampling day and this could have increased DO.

Salinity 11/18/11:

Salinity values measured higher inside the PRB ranging from around 1.0 to 5.0 ppt. Groundwater salinity values dropped to <=0.10 for wells 0-3 (all up-gradient of the PRB) and wells 4 and 5 underneath the PRB (approximately 0.5 meters underneath the PRB). Sampling on 11/18/11 showed that a higher salinity core in the PRB was present down-gradient of well 7 (at 1 meter directly down-gradient of the PRB), seen by increased salinity (Figure 5). A high concentration plume appeared in the deeper zones in wells 4 and 5 (at 1.5 meters underneath the PRB) during the sampling period with values around 8 ppt (Figures 5).

Figure 5. DO in mg/L, salinity in ppt and Cl^- in µM from sampling wells inside, up-gradient, down-gradient and underneath the PRB (indicated by the brown box) on 11/18/11.

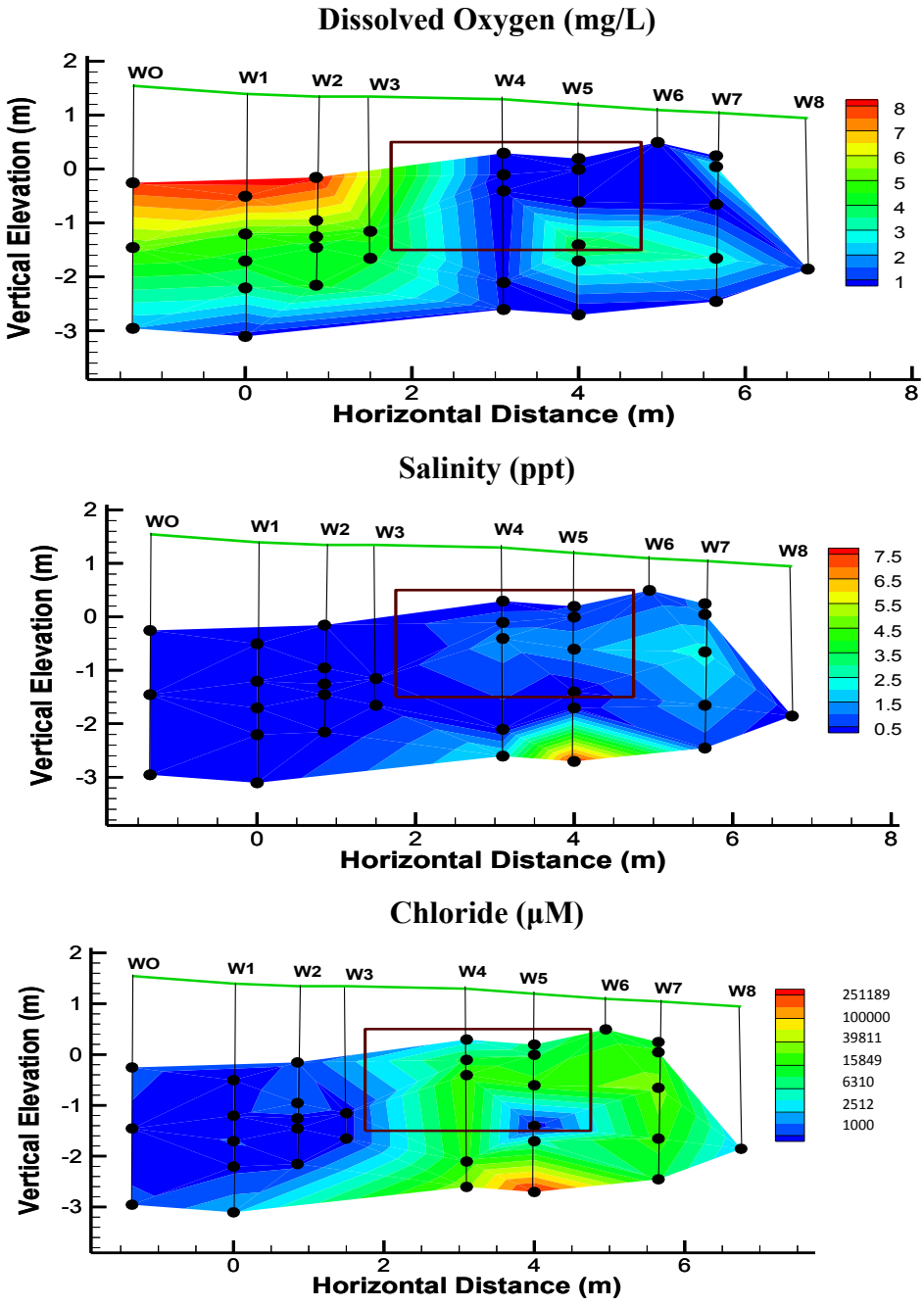

DO 6/7/12 (PRB):

DO was higher up-gradient of the PRB with wells 0, 1 and 2 showing the highest concentrations of around 5-6 mg/L in the upper sampling depths about 1-2 meters directly up-gradient of the PRB (Figure 6). Conditions within the PRB were mostly anoxic with wells 4 and 5 showing DO of less than 1 mg/L for virtually all sampling depths. There was a slight increase in DO down-gradient of the PRB with lower well 7 depths showing DO values ranging from 1 to 3 mg/L.

DO 6/7/12 (Control):

DO values were consistently high throughout the control site with values over 6 mg/L in the upper gradient wells. The middle and lower wells showed values ranging from 4 mg/L to 5 mg/L. The deepest wells contained anoxic conditions with DO values less than 1 mg/L (Figure 6).

Salinity 6/7/12 (PRB):

Up-gradient wells are primarily groundwater fed and showed negligible salinity values. Beginning at well 4 within the PRB, salinity values increased to over 20 ppt in some samples. Salinity continued to stay high down-gradient of the PRB approaching Waquoit Bay. Underneath, salinity values were high as well in the 10-15 ppt range (Figure 6).

Salinity 6/7/12 (Control):

Up-gradient wells were primarily fresh with increasing salinity moving down-gradient. Salinity values peaked around 15 ppt in the deeper wells down-gradient in well

6. Salinity up-gradient ranged from 0-5 ppt while further down-gradient wells measured 5-10 ppt (Figure 6).

Figure 6. DO in mg/L and salinity in ppt from sampling wells within, up-gradient, down-gradient and underneath the PRB (indicated by the brown box) on 6/7/12. Left images indicate PRB site and right images indicate control site.

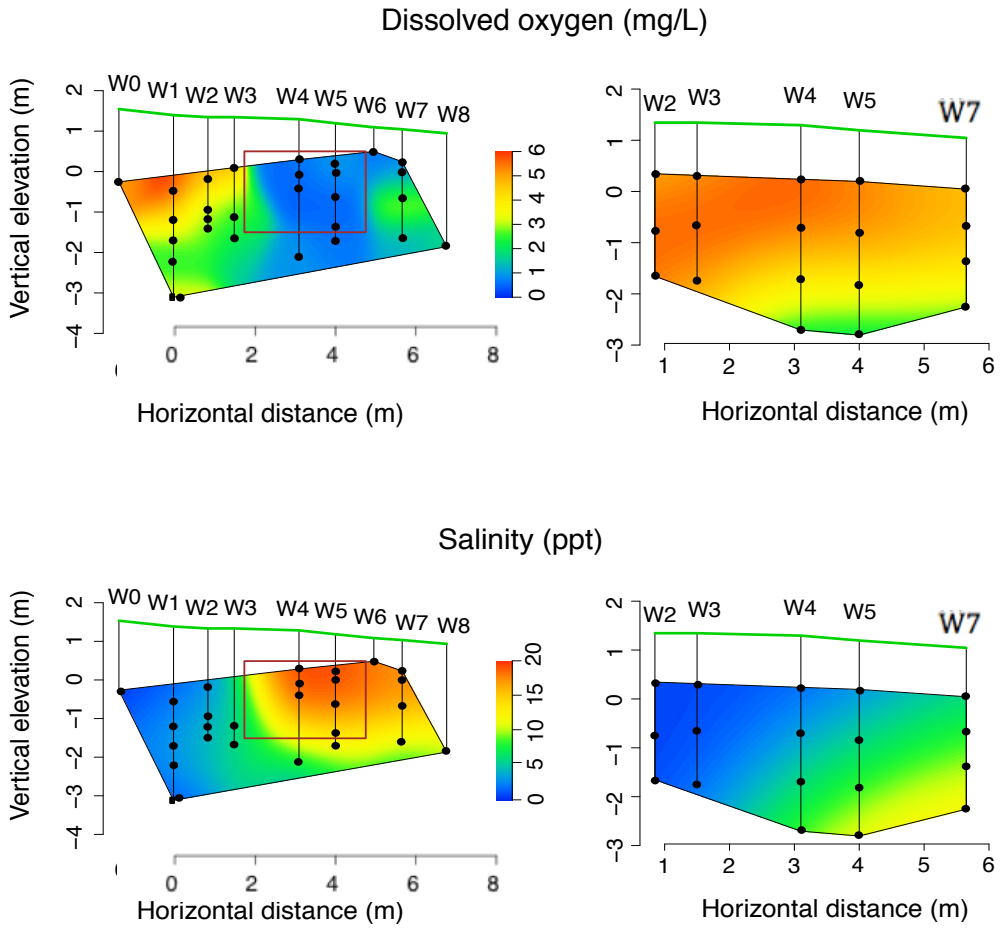

Salinity and DO:

A comparison between DO and salinity from both sampling periods shows a non-linear relationship with the curves falling below linearity. Sampling sites with higher salinity have lower DO concentrations (Figure 7).

Figure 7. The top graph shows salinity concentrations versus DO concentrations from within, up-gradient, down-gradient and underneath the PRB and the control site on 6/7/12. Blue diamonds represent the PRB site and red squares represent the control site. Curve of best fit determines an R^2 of 0.31 for the control site (red squares) and an R^2 of 0.47 for the PRB site (blue diamonds). The bottom graph shows salinity concentrations versus DO concentrations from inside, up-gradient, down-gradient and underneath the PRB on 11/18/11. Curve of best fit shows an R^2 of 0.59.

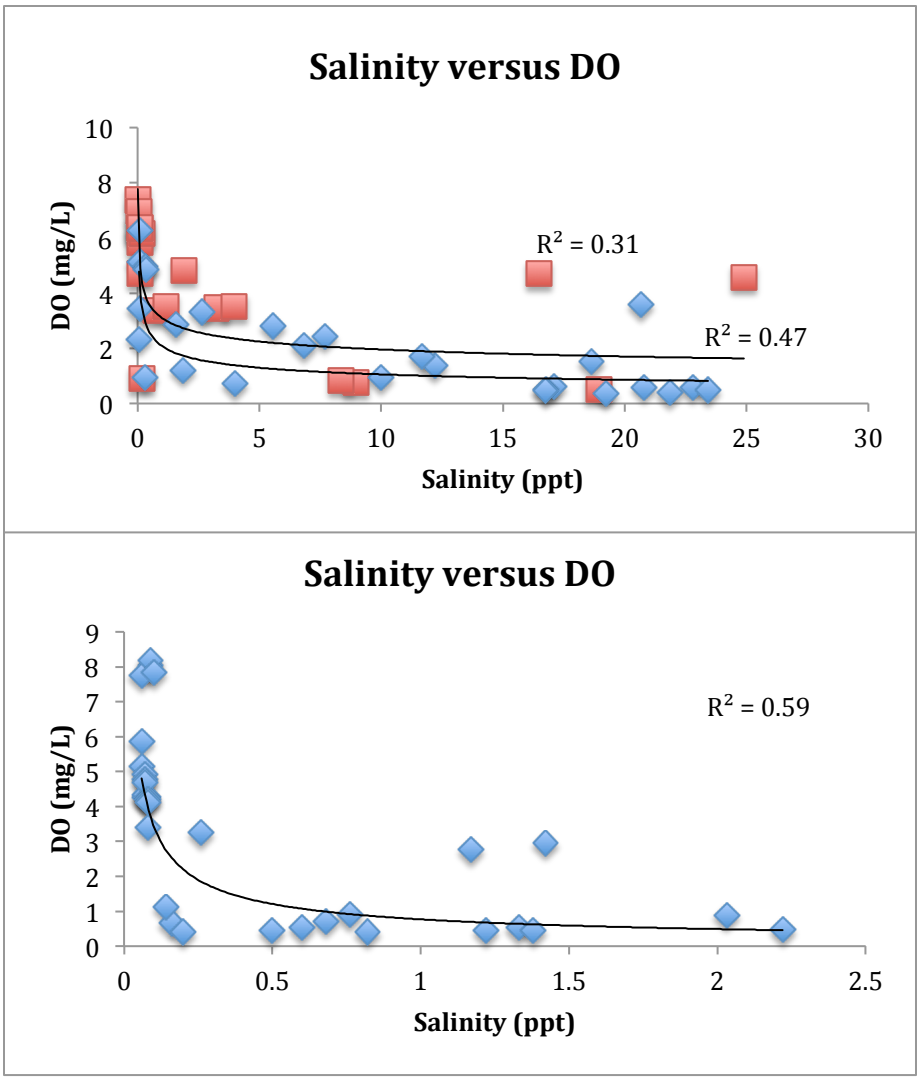

SO_4/ Cl^- / H_2S:

SO_4 and Cl^- concentrations were very similar to one another with concentrations increasing at the start of the PRBs up-gradient side extending to all down-gradient wells in addition to underneath the PRB (Figures 5 and 8). Inside and down-gradient of the PRB, SO_4 concentrations ranged from about 500 μM to 2000 μM, while Cl^- concentrations ranged from about 3000 μM to 40,000 μM. Cl^- and salinity produced a highly correlated relationship with an R^2 of 0.88.

H_2S concentrations were highest inside the PRB and immediately down-gradient of the PRB ranging from 50 to 300 μM (Figure 8). All sites up-gradient and underneath the PRB had extremely low H_2S concentrations (less than 20 μM).

Figure 8. NH_4, NO_3, SO_4, H_2S, DOC and DIC concentrations (µM) in sampling wells inside, up-gradient, down-gradient and underneath the PRB on 11/18/11.

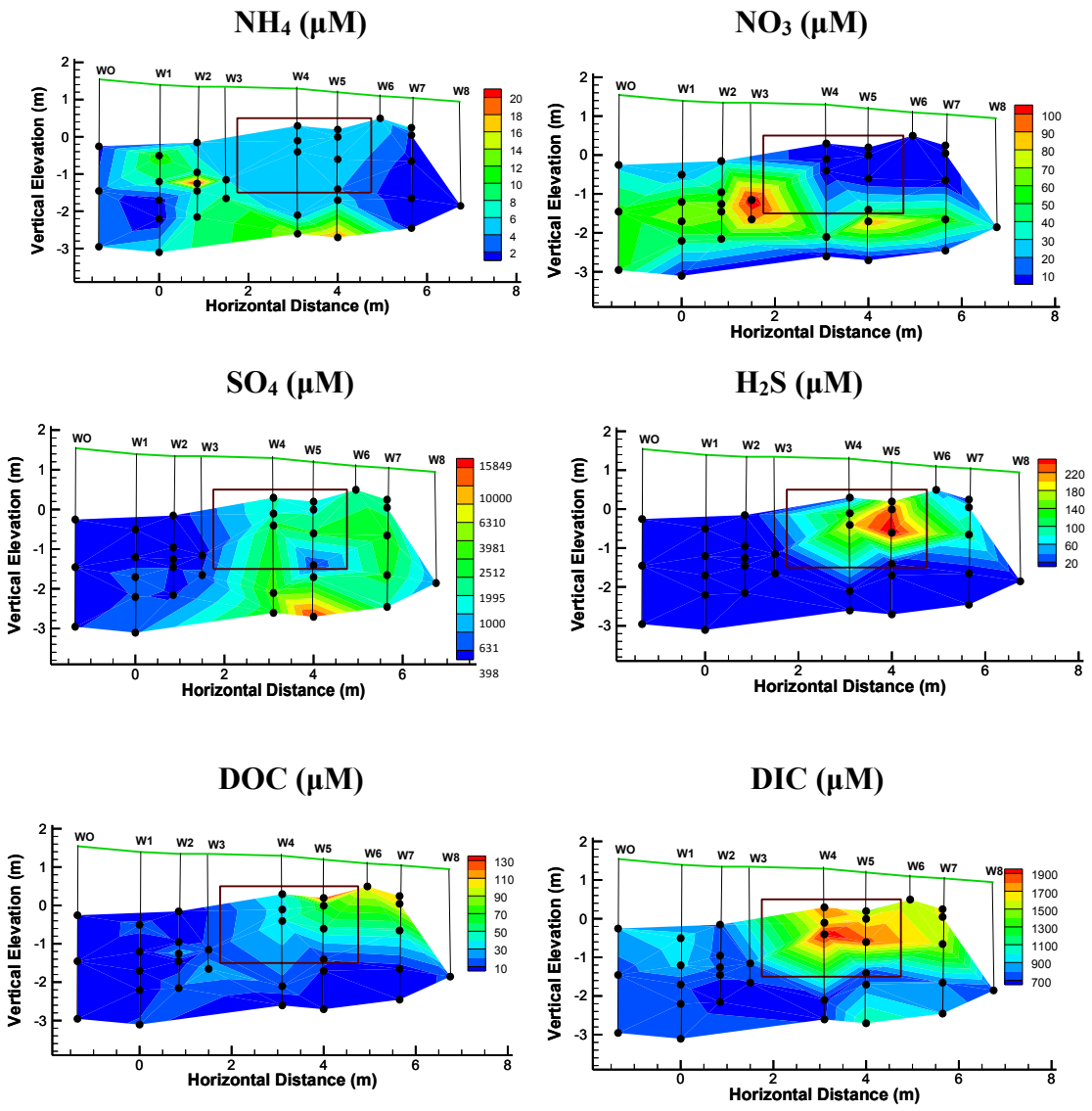

DOC/DIC 11/18/11:

DOC concentrations were highest inside and at wells directly down-gradient of the PRB ranging from 30-130 µM (Figure 8). Low DOC concentrations extended to the wells and sampling depths up-gradient of the PRB with values less than 10 µM. High DOC concentrations did not extend underneath the PRB, but did show clear movement down-gradient.

DIC concentrations follow a similar pattern to DOC concentrations, with the highest values inside and down-gradient of the PRB. Peak concentrations were around 2000 µM inside the PRB and concentrations mostly ranged from around 1000 to 1800 µM inside and down-gradient of the PRB (Figure 8). Wells up-gradient of the PRB and wells underneath the PRB had DIC concentrations around 700 µM with two isolated pockets in well 1 and the lower depths of well 5 with concentrations over 1000 µM. DIC from respiration follows a similar pattern to DIC concentrations with the highest values inside and down-gradient of the PRB, ranging from 400 to 1200 µM in these zones (Figure 9). DIC from respiration was lower up-gradient and underneath the PRB (less than 100 µM).

Figure 9. DIC concentrations from respiration (µM) from sampling wells inside, up-gradient, down-gradient and underneath the PRB on 11/18/11.

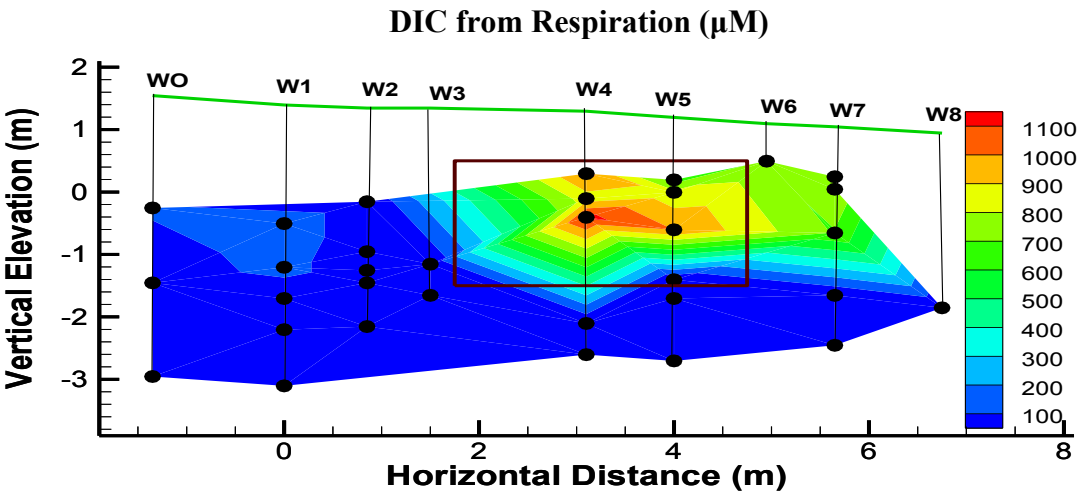

NO_3/ NH_4:

NO_3 concentrations were highest up-gradient of the PRB and underneath the PRB. As expected, the NO_3 concentration dropped to near 0 µM inside most of the PRB and down-gradient (Figure 8). Up-gradient of the PRB, concentrations ranged from around 30 µM to 120 µM, which subsequently dropped to less than 10 µM inside the PRB and

down-gradient. There is a definite plume of high NO_3 concentrations immediately underneath the PRB, extending from the up-gradient wells to well 8 (closest to Waquoit Bay) with a thickness of around 1.5 meters. After reaching well 8 with a depth of 2.75 meters from the beach surface, the NO_3 concentration dropped to around 30 μM. The lowest depths for each of the sampled wells showed low NO_3 concentrations (around 0 μM), similar to concentrations inside the PRB.

NH_4 concentrations peaked up-gradient of the PRB in the middle depths (at 2.5 meters deep) of well 2 at around 20 μM and underneath the PRB in the deeper zones of wells 4 and 5 (Figure 8). NH_4 concentrations inside the PRB remained low and consistent at around 4-6 μM. NH_4 concentrations down-gradient of the PRB were low (less than 2 μM).

Statistical Tests:

Differences in DO, DOC, H_2S, and DIC from respiration were all statistically significant ($p<0.05$) from up-gradient sample sites to PRB influenced and down-gradient sample sites (Figure 10). DO compared to H_2S, DOC and DIC from respiration all produced significant linear regressions with p-values<0.05 (Figure 11). Additionally, H_2S was found to strongly correlate with DOC and DIC from respiration ($p<0.05$) (Figure 12).

Figure 10. The top graph shows a comparison between up-gradient and PRB/down-gradient concentrations of DOC, H_2S and DO. All were statistically significant with p-values<0.05. DOC had a p-value of 0.004, H_2S had a p-value of 0.005, and DO had a p-value of $5.5*10^{-7}$. The bottom graph shows a comparison between up-gradient and PRB/down-gradient concentrations of DIC from respiration. There was statistical significance with a p-value of 0.0003.

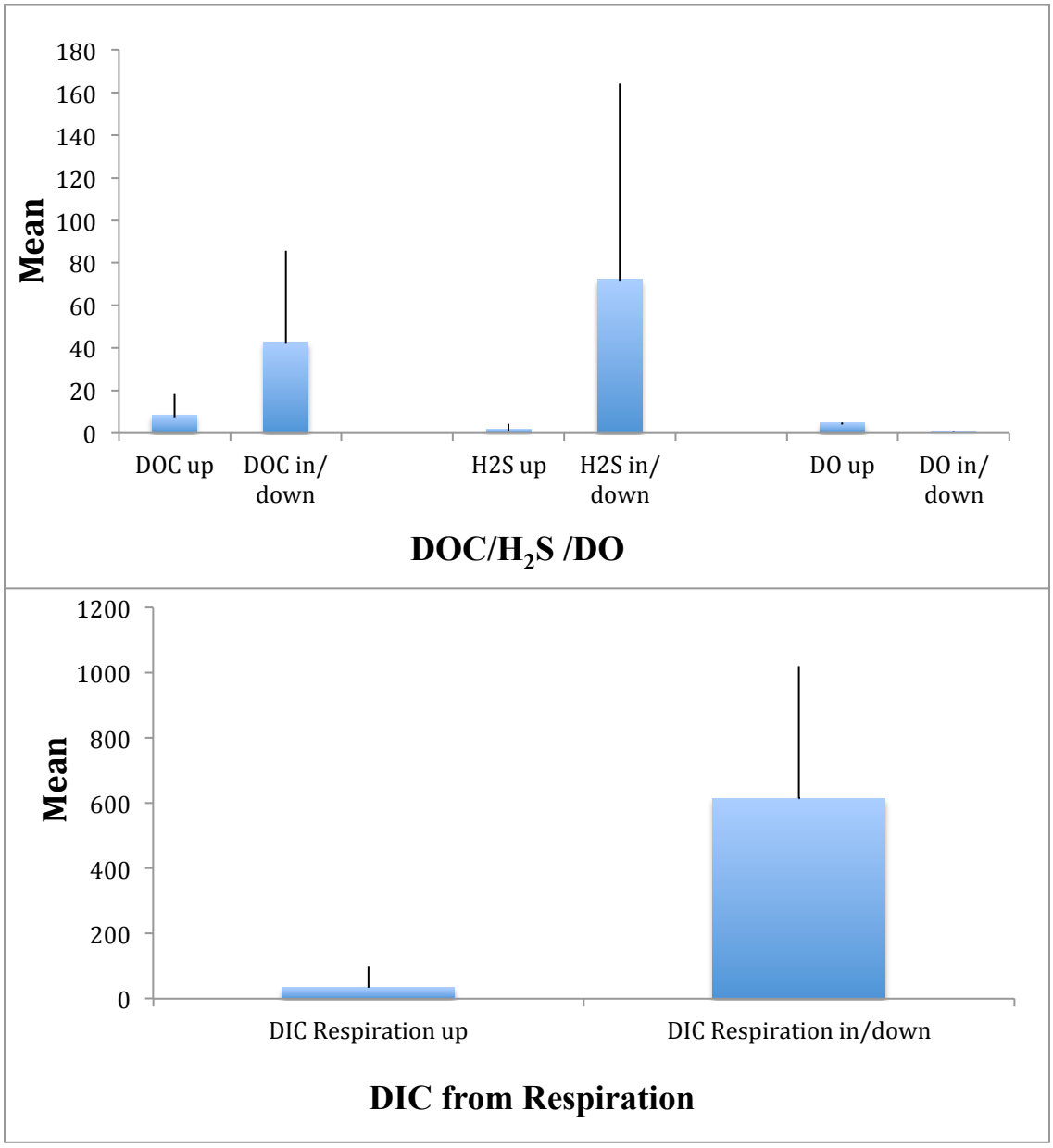

Figure 11. Linear regression analyses of DO in mg/L compared to H_2S, DOC and DIC from respiration. All three analyses with df = 31 were significant with a t-value of 2.82 for DO versus H_2S (p-value = 0.008), a t-value of 2.82 for DO versus DOC (p-value = 0.008), and a t-value of 3.48 for DO versus DIC from respiration (p-value = 0.0015).

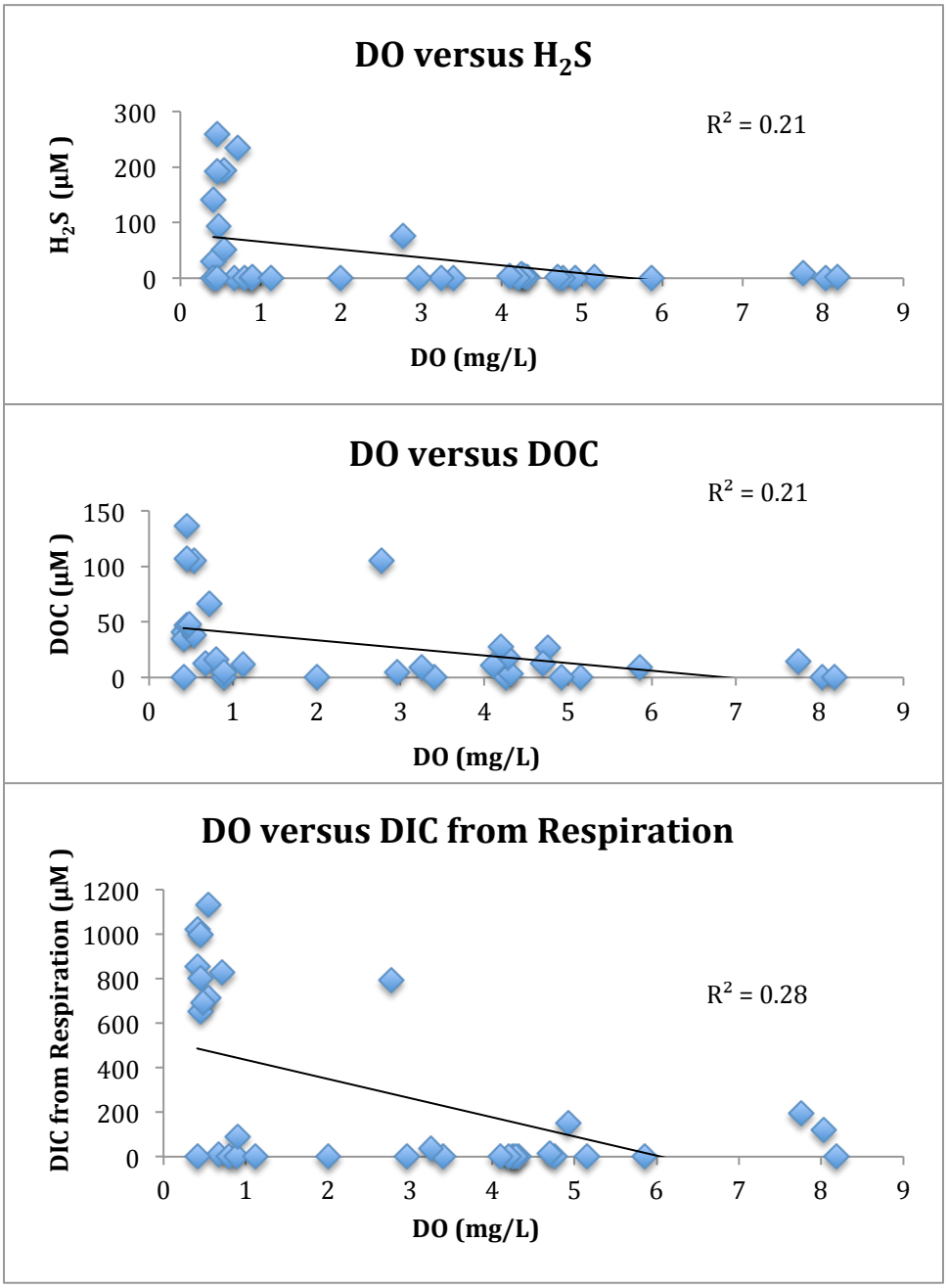

Figure 12. Correlation analyses of H_2S with DOC and DIC from respiration. Both analyses were significant (p-value <0.05) with DOC versus H_2S having a t-value of 6.75 with df=27 and DIC from respiration versus H_2S having a t-value of 7.05 with df=27.

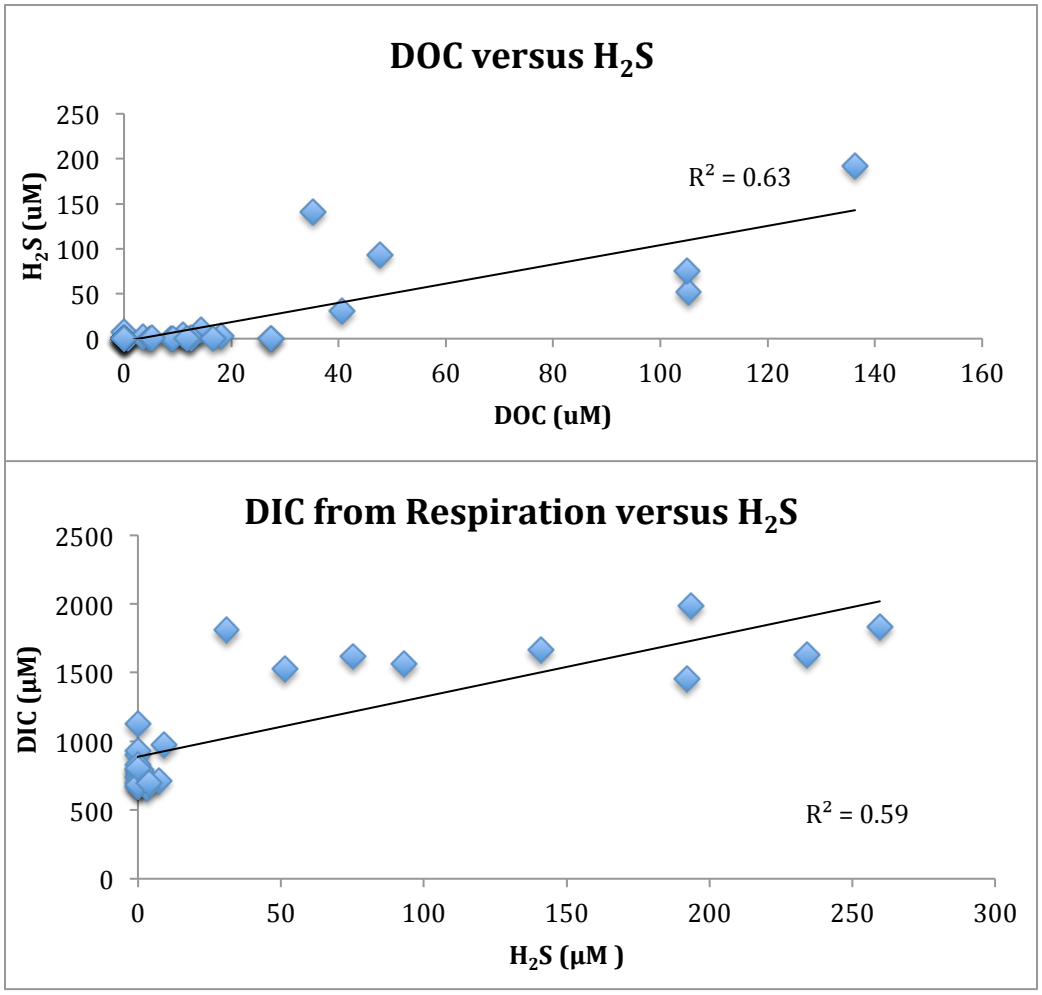

NirS Gene Abundance:

The *nir*S gene was present in every sampling site. The abundance of the *nir*S gene was highest inside and down-gradient of the PRB (Figure 13). Even with the limited sampling sites, clear trends emerged up-gradient, down-gradient, inside and underneath the PRB. The most prolific *nir*S gene region ranged from around 10,000 copies/ng DNA to 35,000 copies/ng DNA and spanned inside the PRB in addition to down-gradient (Figure 13). The abundance dropped up-gradient to around 2000 copies/ng DNA in addition to depths well below the PRB. Differences in *nir*S were statistically significant (p-value <0.05) from up-gradient sample sites to PRB influenced and down-gradient

sample sites (Figure 13). Additionally, there was a significant relationship between DO and *nir*S abundance with a t-value of 3.12 for df = 8 (p-value<0.05) (Figure 14).

Figure 13. The top graph shows the copy number/ng DNA from qPCR in sampling wells inside, up-gradient, down-gradient and underneath the PRB on 11/18/11. The bottom graph shows a comparison between up-gradient and PRB/down-gradient *nir*S abundances. There was statistical significance with a p-value of 0.007.

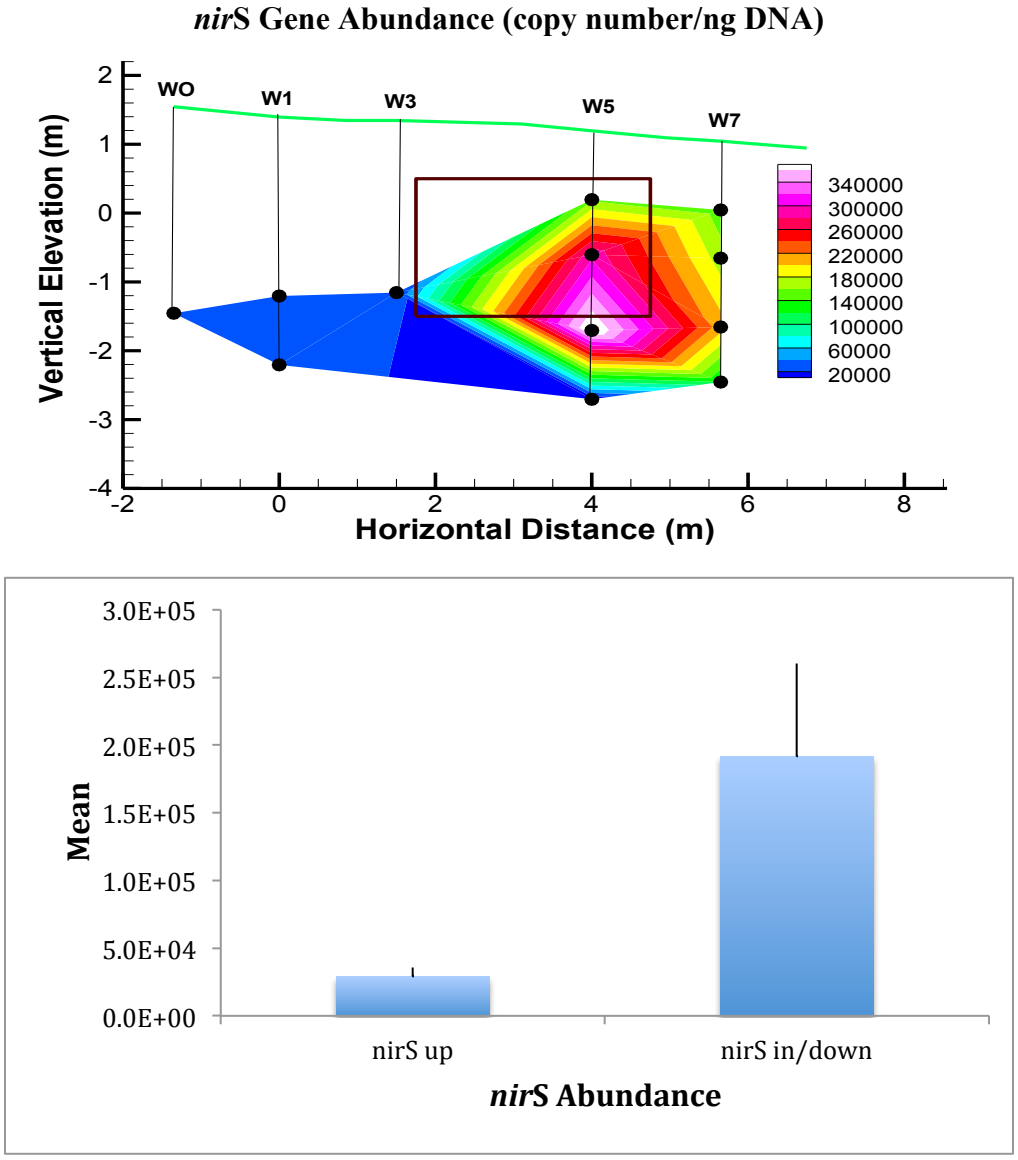

Figure 14. This graph shows *nir*S abundance versus DO from sampling wells inside, up-gradient, and down-gradient of the PRB. Two samples were not included in this figure. The first sample, well 5—2.9 meters, experienced air bubbles from a fractured tube causing higher than expected DO levels. The other sample, well 5—3.9 meters, was located neither up-gradient nor in the PRB/down-gradient and had a *nir*S copy number inconsistent with the system.

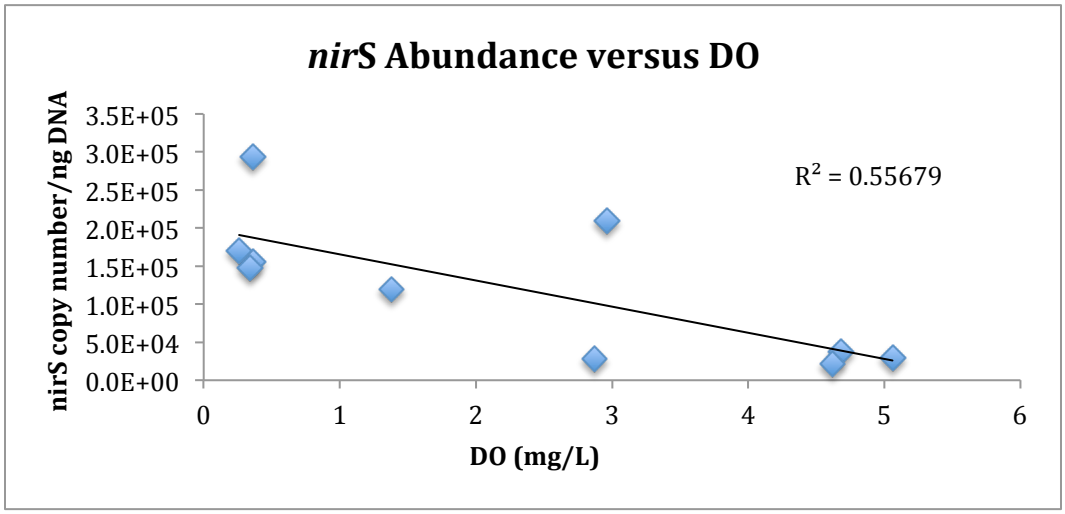

DGGE Analysis:

Whole microbial community composition analysis showed distinct similarity among samples (Figures 15). For example, samples within the PRB shared a high similarity and had a nearly 60% similarity between control samples and up-gradient PRB samples. Within the PRB, there was a 50% similarity among samples just down-gradient and just underneath the PRB belonging to this category. Further down-gradient and underneath samples had a 20% similarity. Control and PRB site samples were separated into three general bacterial groups based on this similarity.

Figure 15. The top figure shows a multidimensional scaling (MDS) plot of microbial community structure in PRB and control wells (see key). The bottom figure shows a cluster analysis of microbial community structure in PRB and control wells (see key).

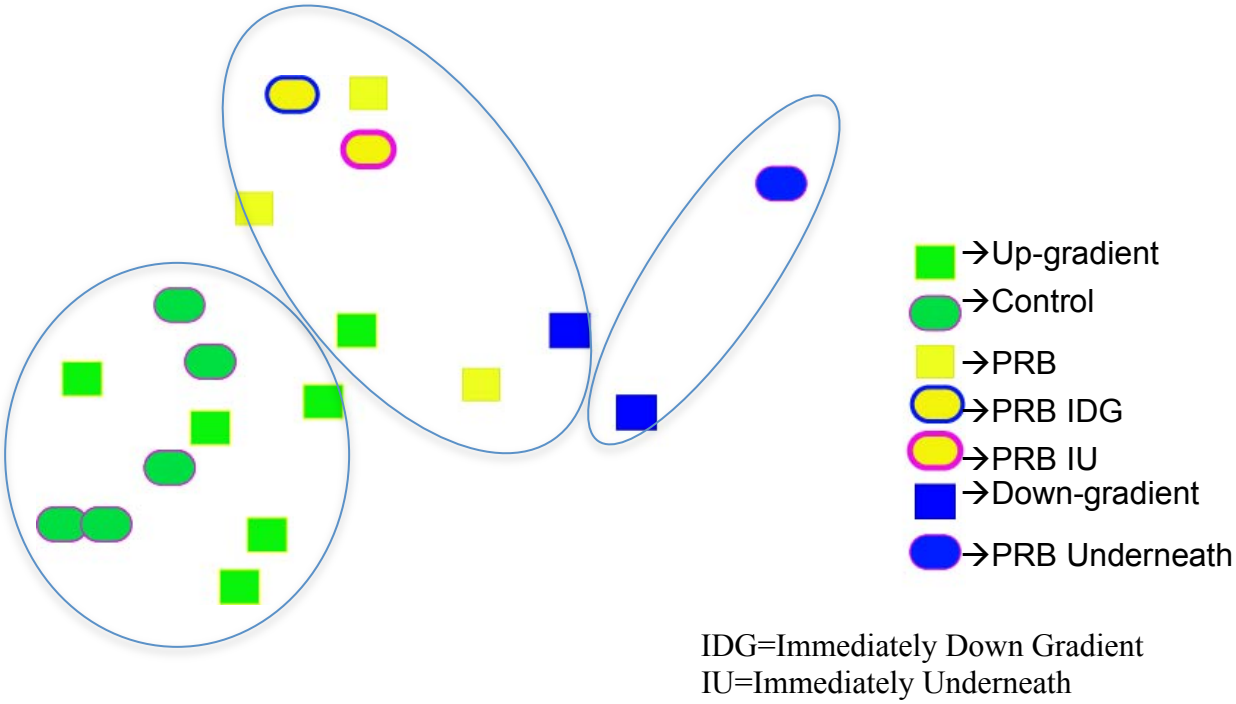

IDG=Immediately Down Gradient
IU=Immediately Underneath

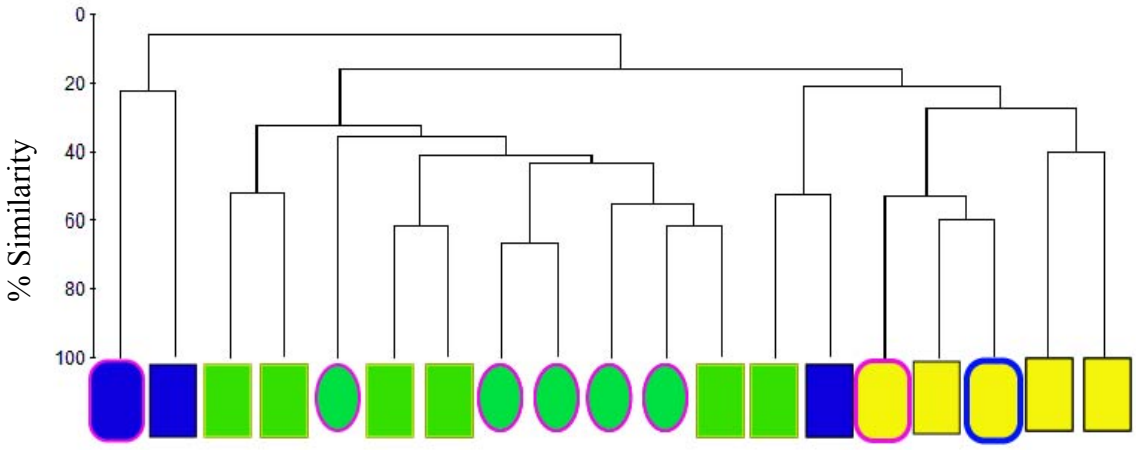

Discussion:

The PRB effectively reduces excessive nitrogen loading into Waquoit Bay through increasing the availability of DOC for denitrifying microbes. In addition, the presence and abundance of denitrifying bacteria assessed using the *nir*S functional nitrite reductase gene was highest in wells and depths with access to increased DOC. This increase in denitrifying microbes coincides with several important biogeochemical changes occurring as a result of the PRB. The successful reduction of NO_3 from contaminated groundwater (Figure 8) and the presence of suboxic zones within the PRB (Figure 5) suggest that an adequate environment for denitrification has been achieved with the microbes within the PRB metabolizing the carbon rich wood chip media. With noticeable biogeochemical changes within the PRB, whole microbial community analysis using DGGE additionally revealed distinct groups with genetic similarity between the PRB and control sites. An increase in organic matter content coupled with NO_3-rich groundwater and low DO levels should encourage strictly anaerobic phylotypes with denitrifiers dominating (Huang et al., 2011).

In looking at the effectiveness in removing NO_3 from the groundwater, my results show that the PRB was successful in reducing most NO_3 that entered the PRB itself due to the presence of denitrifying conditions. As seen in figure 10, concentrations of DOC, H_2S, DO and DIC from respiration changed significantly from up-gradient sample sites to PRB influenced/down-gradient sample sites. This strongly suggests that the PRB affects the cycling and movement of nutrients within this experimental system. However, even with these biogeochemical alterations and elimination of NO_3, there is a NO_3 enriched plume passing underneath the PRB (Figure 8). With low NO_3 concentrations persisting

in the deepest wells, it appears that the NO_3-rich groundwater passing underneath the PRB sits between a saline top layer and saline bottom layer (Figures 5 and 8). This is supported by the salinity concentrations, which increased inside and down-gradient of the PRB and in the deeper wells underneath the PRB.

During the June 2012 sampling period, in which the salinity concentrations were greatly increased compared to the November 2011 sampling, there was a question as to whether or not the PRB was reducing NO_3, or whether the frequent high tide seawater inundations were diluting NO_3 from the samples (Figure 6). A comparison between salinity and DO concentrations during the November 2011 and June 2012 sampling suggests there are other contributing factors to suboxic conditions in the PRB site than seawater diluting the NO_3 concentrations before it enters the Bay. If this were due to a dilution factor, then there would be a linear relation between these measurements. However, both curves in figure 7 fall below linearity, meaning another factor, such as the PRB, is removing additional DO from the groundwater. Additionally, the porous sediment structure created by the wood chip media would enable increased seawater infiltration. This was supported by the salinity concentrations, which increased within and down-gradient of the PRB and in the deeper wells underneath the PRB (Figures 5 and 6). Some have suggested that the mixing between these saline and groundwater layers is a dominant transport mechanism for nutrients such as NO_3 to enter coastal ecosystems (Moore, 1996; Moore, 1999). However, even with fresh groundwater and saline seawater mixing, research has shown this occurrence contributes very little nutrients to coastal ecosystems (Weinstein et al., 2010).

Even with the deeper plume of NO_3 underneath the PRB, a prior study has shown that PRB systems effectively remove NO_3 from groundwater (Robertson et al., 2000). After a 2006 study by Angela Vincent, in which low NO_3 concentrations showed their effective removal before entering Waquoit Bay, the development of a deeper NO_3 plume also occurred (Vincent, 2006). Previous studies have shown the importance of external carbon sources on aquatic ecosystems in altering nitrogen dynamics (Bernhardt and Likens, 2002), and it is often contingent on carbon being sufficiently labile to contribute to denitrification (Robertson et al., 2000). Further, in previous studies, successful denitrification was often affected by several factors including NO_3 concentration, organic matter content and DO (Dong et al., 2009). Therefore, I predicted that movement of necessary DOC down-gradient coincided with increased abundance of the *nir*S gene. Since NO_3 entering the Bay down-gradient of the PRB have consistently measured low concentrations, the presence and abundance of the *nir*S gene in down-gradient locations would support NO_3 removal down-gradient of the PRB.

My results show that the *nir*S nitrite reductase gene increased in abundance inside and down-gradient of the PRB, indicating the effectiveness of DOC in supplying denitrifying bacteria with a carbon source. In fact, the NO_3 plume (Figure 8) seems to undercut the high abundance of *nir*S inside the PRB but further diminishes once the *nir*S abundance remains high down-gradient of the PRB. These results suggest the potential of a NO_3 plume flowing underneath the PRB being intercepted by down-gradient denitrifying bacteria that are feeding off of increased DOC from the wood chip matrix decomposition inside the PRB. Previous studies have shown that the distribution of denitrifying genes in sediments is affected by several factors including NO_3

concentration, organic matter content and DO (Dong et al., 2009). With an increase in organic matter content coupled with NO_3-rich groundwater and low DO levels, the diverse anaerobic denitrifiers should dominate the microbial community (based on *nir*S diversity) (Huang et al., 2011). Further, a comparison between *nir*S abundance and DO from the PRB shows that denitrifying microbes inhabited oxygen-rich and anoxic zones ranging from <=1 mg/L to over 5 mg/L of DO, however there was a strong preference for anoxic conditions with much greater *nir*S copy numbers (Figure 14). Further, there was a significant change in *nir*S abundance from up-gradient locations to PRB/down-gradient locations (Figure 13). Therefore, denitrifying microbes not only are present within the PRB, but down-gradient as well, indicating a more expansive overall denitrification effectiveness.

In a recent study looking at functional genes and denitrification rates in aquatic sediments, denitrification peaks coincided with peaks in *nir*S gene abundance (Unpublished Abstract, Bowen et al., 2010). The success of the PRB in providing a carbon source for denitrifiers combined with the definite movement of DOC down-gradient allows denitrification to persist efficiently outside of the PRB itself. Interestingly, with the low abundance of the *nir*S gene in wells below the PRB, it appears that the movement and success of denitrifying bacteria extends horizontally down-gradient of the PRB but not vertically below. In order to gather a more complete profile of *nir*S abundance down-gradient of the PRB, more sampling wells are needed in addition to characterization of specific denitrifying microbes (e.g. through sequencing).

The statistical significance of the increased DIC from respiration inside and down-gradient of the PRB also supports the idea that increased metabolic activity of

microbes as a result of higher DOC concentrations is associated with the removal of NO_3 by denitrification (Figure 9). However, the amount of excess DIC from respiration indicates other anaerobic decomposition pathways, such as fermentation and SO_4 reduction (*personal communications*, Foreman). Prior studies have shown that anaerobic microbes drive much of the carbon remineralization in aquatic ecosystems and that there should be associated DIC from respiration increases in systems having abundant DOC available (Sampou and Oviatt, 1991). Additional research supports anaerobic microbes dominating benthic metabolisms due to greater carbon remineralization relative to sedimentary oxygen consumption (Zimmerman and Benner, 1994). Zimmerman and Benner found that DIC production measurements were useful in consistently estimating total integrated rates of carbon remineralization. Aquatic ecosystems experiencing eutrophication alter carbon and energy cycling as a result of increased organic sedimentation and as a result, the importance of anaerobic respiration increases (Mackin and Swider, 1989). My results show that DIC concentrations from respiration were much higher inside the PRB and down-gradient of the PRB, suggesting that microbial community metabolisms have increased in these zones (Figure 9).

Overall, my results show higher DOC concentrations in sampling sites with lower DO concentrations and these concentrations also correlated using a linear regression analysis (Figure 11). In addition, I found lower average *nir*S abundances in sites with higher DO (Figure 14). Lower DOC concentrations showed variability between oxic and anoxic conditions and the higher concentrations (greater than 40 μM) were exclusively anoxic. This indicates the importance of DOC in driving microbial metabolism to

exhaust oxygen and create conditions suitable for denitrification to occur and the importance of the PRB in providing these conditions of high carbon and low oxygen.

During the November 2011 sampling period, the presence of seawater intrusion inside the PRB can be seen by the SO_4, H_2S and salinity contours (Figures 5 and 8). While my measurements do not show seawater intrusion as prominently as Angela Vincent's research, the high concentration of H_2S in the center of the PRB combined with low DO concentrations indicates the presence of SO_4 reducers that reduce dissolved SO_4 and compete against anaerobic respiration processes such as denitrification in organic-rich marine sediments (Vincent, 2006; Brüchert et al., 2003). Further, during the June 2012 sampling period, the presence of seawater intrusion within the PRB can be seen by the salinity contours (Figure 6) with much higher concentrations of saline seawater inundating the PRB and potentially introducing SO_4 to the carbon-rich environment. Studies have supported the incidence and magnitude of SO_4 reduction as a by-product of the carbon available in the surrounding space. In fact, SO_4 reduction has been shown to vary as much as eight orders of magnitude in marine sediments depending of the quality and amount of a labile, carbon source (Westrich and Berner, 1984).

Prior studies have shown that SO_4 reduction may contribute over half of mineralized carbon in marine sediments (Leloup et al., 2004). Comparisons between H_2S and DIC from respiration and H_2S and DOC show positive correlations (Figures 12). Therefore, SO_4-reducing bacteria likely assimilate and therefore deplete a portion of the labile DOC from the PRB and contribute to the total respired DIC from the PRB. Further, a linear regression analysis shows that a correlation between high H_2S concentrations and low DO concentrations is statistically significant (Figure 11). With a

labile carbon source from the PRB, suitable anoxic conditions, and high concentrations of H_2S within the PRB, it is likely SO_4-reducing bacteria play an important role in the PRB dynamics.

In order to get a better understanding of the nature of NO_3 and SO_4-reducing microbes in the PRB, a competition study is recommended to determine the potential effects of seawater intrusion on DNRA and denitrification. Furthermore, the complexity of the denitrification pathway in a sulfidic system like that created by the PRB necessitates analysis on sulfur oxidizers, which may assimilate a significant portion of the NO_3 present through assimilation. If this is the case then nitrogen cycling would be carefully linked to H_2S availability and therefore SO_4 reduction, supporting the notion that seawater intrusion might not be as detrimental to the PRB's efficacy as currently believed (Burgin and Hamilton, 2007).

While NH_4 concentrations remained relatively constant inside the PRB, they were higher than down-gradient concentrations and suggest that DNRA may be occurring (Gilbert et al., 2008). Increased SO_4 from seawater (Figure 5) may be intensifying the DNRA process, resulting in production of NH_4 that is either converted back to NO_3 via nitrification in aerobic environments or assimilated biologically into plant or microbial biomass (Burgin and Hamilton, 2007). Considering H_2S inhibition of the final two steps of denitrification may push reduction to NH_4 rather than to N_2 gas, a system infiltrated by SO_4 and H_2S should express clear DNRA, however the NH_4 concentrations in the PRB measure low values that may lessen the current effect of seawater intrusion on DNRA. A future experiment could also look for and measure the concentration of metal bound sulfides (e.g. iron sulfide), which are often abundant but may not inhibit denitrification

(Burgin and Hamilton, 2007). Another interesting area of research might be quantifying the effect of seawater on DNRA inside the PRB and tracking the movement of NH_4 products of DNRA down-gradient.

The high DOC concentrations and metabolic activity represented by DIC from respiration combined with the increased abundance of the denitrification *nir*S gene inside and down-gradient of the PRB represents the potential for denitrification. Additionally, high DOC and metabolic activity may be leading to the attenuation of the NO_3 plume underneath the PRB as well as the portion of the plume directly impinging on the PRB. Finally, the presence of SO_4-reducing bacteria inside the PRB indicates resource competition (e.g. DOC) with denitrifiers.

Whole microbial community analysis of the PRB and control sites produced unique differences. The high similarity among the samples within the PRB suggests the altered biogeochemistry has created favorable conditions for certain microbes (Figure 15). Further, the dissimilarity between the PRB microbial communities and those up-gradient support a changing microbial community structure as a result of the PRB. When compared to the control samples, the presence of a PRB becomes clearer. All control samples have a high similarity to the up-gradient samples, but not to the PRB samples. Therefore, one could predict that with no PRB, the microbial community that would exist where the PRB is located should resemble the microbial community at the control site. Additionally, the high similarity between the control samples and the up-gradient samples suggests that the PRB does not have a significant up-gradient effect on the microbial diversity. After well 3 in the PRB site, however, a differentiation from the control site's microbial diversity occurred, and this is likely due to the altered biogeochemistry from

the external carbon and the inundating seawater. This suggests that the PRB has a direct influence on the presence or absence of certain microbial communities. Interestingly, the sample underneath the PRB and the sample from well 8 (furthest down-gradient well) showed distinct dissimilarity from the up-gradient and PRB communities. This could be attributed to unique biogeochemical conditions occurring in the lower saline region underneath the PRB and the more saline region closer to the Bay.

Acknowledgements:

From Colorado College, I would like to thank my advisors Drs. Mark Wilson and Miroslav Kummel for their guidance throughout the writing process. From the Woods Hole Marine Biological Laboratory, I would like to thank my advisor Dr. Kenneth Foreman for his valuable advice and support throughout the project and for joining me in the field to collect samples during the fall of 2011 and the summer of 2012. I would also like to thank Dr. Joseph Vallino for fueling my initial interest in the PRB and for helping me use the Tecplot Focus graphing software. I would also like to thank Dr. Julie Huber from the Josephine Bay Paul Center for assisting in the molecular laboratory techniques this project required. Thank you to Emily Reddington, Nancy Akerman, Leslie Murphy and everyone else who helped with DNA extraction and PCR at the Josephine Bay Paul Center. I also thank fellow Woods Hole Semester in Environmental Science student Sarah Nalven, who worked long hours with me during the molecular methods portion of the project. I am incredibly grateful for the amazing Woods Hole TAs—Rich McHorney, Stefanie Strebel, Laura Van der Pol and Carrie Harris—who assisted me throughout the fall of 2011 on lab techniques and data analysis. From the University of Massachusetts Boston REU, I want to thank my research advisor Dr. Jennifer Bowen for her tireless

help throughout the entire process. I also thank Kenly Hiller, Patrick Kearns and Sarah Feinman for their assistance in collecting and analyzing data. I would like to thank Dr. Alan Christian for making my 2012 summer research possible. Thanks to Dr. Dave Weisman for his help with Rstudio and Dr. Michael Shiaris for letting me use his lab for DGGE analysis. This program, CREST REU UMass Boston, was funded by National Science Foundation Award # 1062374 to Hannigan and Christian [OCE-GEO/OCE-Education and Human Resources (Ocean Sciences)]. Finally, I thank my parents for supporting me throughout this project.

Works Cited

Bernhardt, E. S., and G.E. Likens. 2002. Dissolved organic carbon enrichment alters nitrogen dynamics in a forest stream. Ecology **83**(6): 1689-1700.

Braker, G., J. Zhou, L. Wu, A.H. Devol, and J.M. Tiedje. 2000. Nitrite reductase genes (nirK and nirS) as functional markers to investigate diversity of denitrifying bacteria in Pacific northwest marine sediment communities. Appl. Environ. Microbiol **66**: 2096-2104.

Braker, G., A. Fesefeldt, and K.P. Witzel. 1998. Development of PCR primer systems for amplification of nitrite reductase genes (nirK and nirS) to detect denitrifying bacteria in environmental samples. Appl. Environ. Microbiol **64**: 3769-3775.

Brüchert, V., B.B. Jorgensen, K. Neumann, D. Riechmann, M. Schlosser and H. Schulz. 2003. Regulation of bacterial sulfate reduction and hydrogen sulfide fluxes in the central Namibian coastal upwelling zone. Geochimica et Cosmochimica Acta **67**: 4505-4518.

Bowen, J. L., B. B. Ward, H. G. Morrison, J. E. Hobbie, I. Valiela, L. A. Deegan, and M. L. Sogin. 2011. Microbial community composition in sediments resists Perturbation by nutrient enrichment. The ISME Journal 1-9.

Bowen, J. L., B. C. Crump, L. A. Deegan, and J. E. Hobbie. 2009. Response of salt marsh sediment bacteria to external nitrogen inputs as measured by denaturing gradient gel electrophoresis. The ISME Journal **3**: 924-934.

Bowen, J., and I. Valiela. 2001. The ecological effects of urbanization on coastal

watersheds: historical increases in nitrogen loads and eutrophication of Waquoit Bay estuaries. Canadian Journal of Fisheries and Aquatic Science **58**: 1489-1500.

Brunet, R., and L. Garcia-Gil. 1996. Sulfide-induced dissimilatory nitrate reduction to ammonia in anaerobic freshwater sediments. FEMS Microbiology Ecology **21**: 131-138.

Burgin, A. J., and S. K. Hamilton. 2007. Have we overemphasized the role of denitrification in aquatic ecosystems? A review of nitrate removal pathways. Front Ecol Environ **5**(2): 89-96.

Crump, B. C., C. S. Hopkinson, M. L. Sogin, and J. E. Hobbie. 2004. Microbial biogeography along an estuarine salinity gradient: combined influences of bacterial growth and residence time. Appl. Environ. Microbiol. **70**: 1494-1505.

Dong, L.F., C.J. Smith, S. Papaspyrou, A. Stott, A.M. Osborn, and D.B Nedwell. 2009. changes in benthic denitrification, nitrate ammonification, and anammox process rates and nitrate and nitrite reductase gene abundances along an estuarine nutrient gradient (the Colne Estuary, United Kingdom). Appl. Environ. Microbiol **75**: 3171-3179.

Feinberg, D.S. 2010. Wood decomposition after five years in anaerobic nitrate rich groundwaters: implications for lifetime of NITREX™ permeable reactive barriers. Final SES Project. Marine Biological Laboratory.

Gilbert, O., S. Pomierny, I. Rowe, and R.M. Kalin. 2008. Selection of organic substrates as potential reactive material for use in a denitrification permeable reactive barrier (PRB). Bioresource Technology **99**: 7587-7596.

Huang, S., C. Chen, Q. Wu, R. Zhang, and X. Yang. 2011. Distribution of typical denitrifying functional genes and diversity of the nirS-encoding bacterial community related to environmental characteristics of river sediments. Biogeosciences Discuss **8**: 5251-5280.

Jayakumar A, S.W.A Naqvi, and B.B. Ward. 2009. Distribution and relative quantification of key genes involved in fixed nitrogen loss from the Arabian Sea oxygen minimum zone. In: Hood, RR (ed.), Indian Ocean Biogeochemical Processes and Ecological Variability. American Geophysical Union 187–203.

Jones, C.M. "Denitrification: from genes to ecosystems". Ph.D. dissertation. Uppsala University, 2010.

Karr, E.A., W.M. Sattley, M.R. Rice, D.O Jung, M.T. Madigan and L.A. Achenbach. 2005. Diversity and distribution of sulfate-reducing bacteria in permanently frozen Lake Fryxell, McMurdo Dry Valleys, Antarctica. Appl. Envrion. Microbiol. **71**: 6353-6359.

Knauss, C. R. 2011 Characterizing Microbial Denitrification nirS Gene Abundance and Biogeochemical processes up-gradient, within and down-gradient from a NITREX^{TM} permeable reactive barrier in Waquoit Bay, MA. Final SES Project. Marine Biological Laboratory.

Leloup, J., L. Quillet, T. Berthe, and F. Petit. 2006. Diversity and the dsrAB (dissimilatory sulfite reductase) gene sequences retrieved from two contrasting mudflats of the Seine estuary, France. FEMS Microbiology Ecology **55**: 230-238.

Lucey, K. 2006. Permeable reactive barriers as long-term solutions for groundwater remediation: concentrations of methane and dissolved inorganic carbon as indicators of the rates of carbon oxidation processes across the NITREX™ permeable reactive barrier in Waquoit Bay, Cape Cod. Final SES Project. Marine Biological Laboratory.

National Acadamy of Sciences. 2000. Clean coastal waters: Understanding and reducing the effects of nutrient pollution. R.W. Howarth, et al., editors. National Acadamy Press, Washington, DC, USA.

Mackin, J.E., and K.T. Swider. 1989. Organic matter decomposition pathway and oxygen consumption in coastal marine sediments. Journal of Marine Research. **47**: 681-718.

Moore W.S. 1996. Large groundwater inputs to coastal waters revealed by Ra enrichments. Nature **380**: 612-614.

Moore, W.S. 1999. The subterranean estuary: a reaction zone of ground water and sea water. Marine Chemistry **65**: 111-125.

Nogales, B., K.N. Timmis, D.B. Nedwell, and A.M. Osborn. 2002. Detection and diversity of Expressed denitrification genes in estuarine sediments after reverse transcription-PCR amplification from mRNA. Applied and Environmental Microbiology 5017-5025.

Robertson,W.D., D.W. Blowes, C.J. Ptacek, and J.A. Cherry. 2000. Long-term performance of a in situ reactive barriers for nitrate remediation. Ground Water **38:** 689-695.

Robertson,W.D., G.I. Ford, and P.S. Lombardo. 2005a. Wood-based filter for nitrate removal in septic systems. Transactions of the ASAE **48**(1): 121-128.

Robertson,W.D., N. Yeung, P.W. van Driel, and P.S. Lombardo. 2005b. High permeability layers for remediation of ground water; go wide, not deep. Ground Water **43**(4): 574-581.

Sampou, P., and C.A. Oviatt. 1991. A carbon budget for a eutrophic marine ecosystem and the role of sulfur metabolism in sedimentary carbon, oxygen and energy dynamics. Journal of Marine Research **49**: 825-844.

Schipper, L.A., W.D. Robertson, A.J. Gold, D.B. Jaynes, and S.C. Cameron. 2010. Denitrifying bioreactors—an approach for reducing nitrate loads to receiving waters. Environmental Ecology 1532-1543.

Serveiss, V., J. Bowen, D. Dow, and I. Valiela. 2004. Using ecological risk assessment to identify the major anthropogenic stressor in the Waquoit Bay watershed, Cape Cod, Massachusetts. Environmental Management **33**: 730-740.

Solarzano, L. 1969. Determination of ammonium in natural waters by phenol hypochlorite method. Limnol. Oceanogr **14**: 799-800.

Vincent, A. 2006. The Effects of Seawater Intrusion on Microbial Nitrate and Sulfate Reduction within a NITREX^{TM} Permeable Reactive Barrier Designed to Mitigate Groundwater N-Pollution. Final SES Project. Marine Biological Laboratory.

Weinstein, Y., B Herut, Y. Shalem, Y. Yecheili, W. Burnett and P. Swarzenski. 2010. The role of groundwater and recirculated seawater in the transport of nutrients to the coastal water, a case study from the Carmel Coast, Israel. Rapp. Comm. int. 78.

Westrich, J.T., and R.A. Berner. 1984. The role of sedimentary organic matter in Bacterial sulfate reduction: The G model tested. Limnol Oceanogr. **29**: 236-249.

Wood, E.D., F.A.G. Edwards, and F.A. Richards. 1967. Determination of nitrate in seawater by cadmium-copper reduction to nitrite. Journal of the Marine Biological Association of the U.K **47**: 23.

Zimmerman, A.R., and Benner, R. 1994. Denitrification, nutrient regeneration and carbon mineralization in sediments of Galveston Bay, Texas, USA. Mar. Ecol. Prog. Ser **114**: 275-288.

Appendix

Appendix 1. Salinity (ppt) in sampling wells inside, up-gradient, down-gradient and underneath the PRB on 11/14/11.

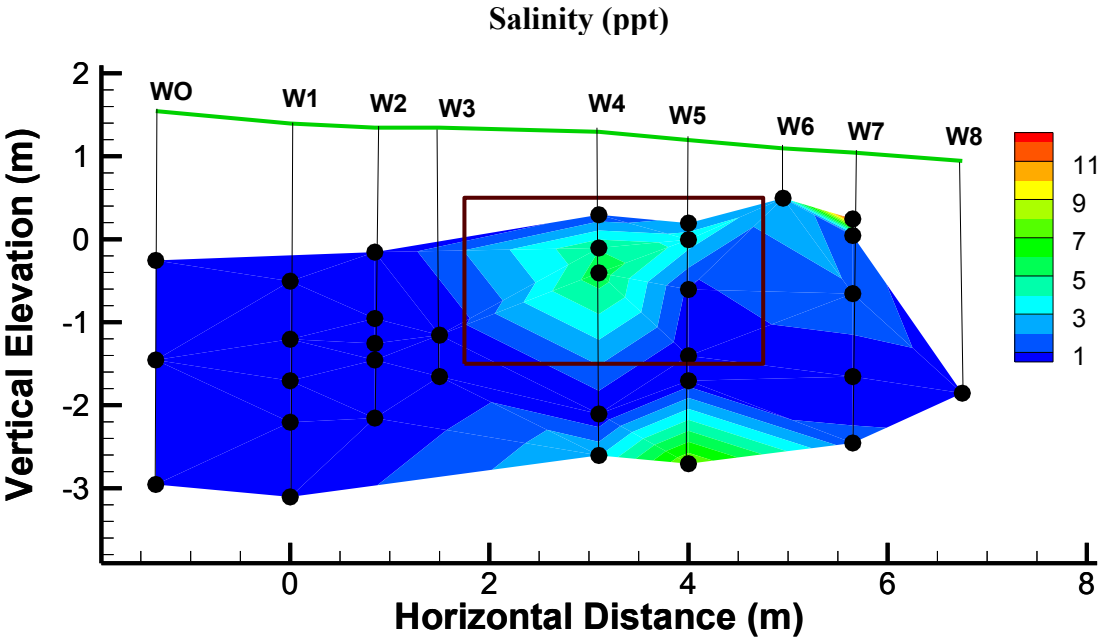

Appendix 2. Phosphate concentrations (µM) from sampling well inside, up-gradient, down-gradient and underneath the PRB on 11/18/11.

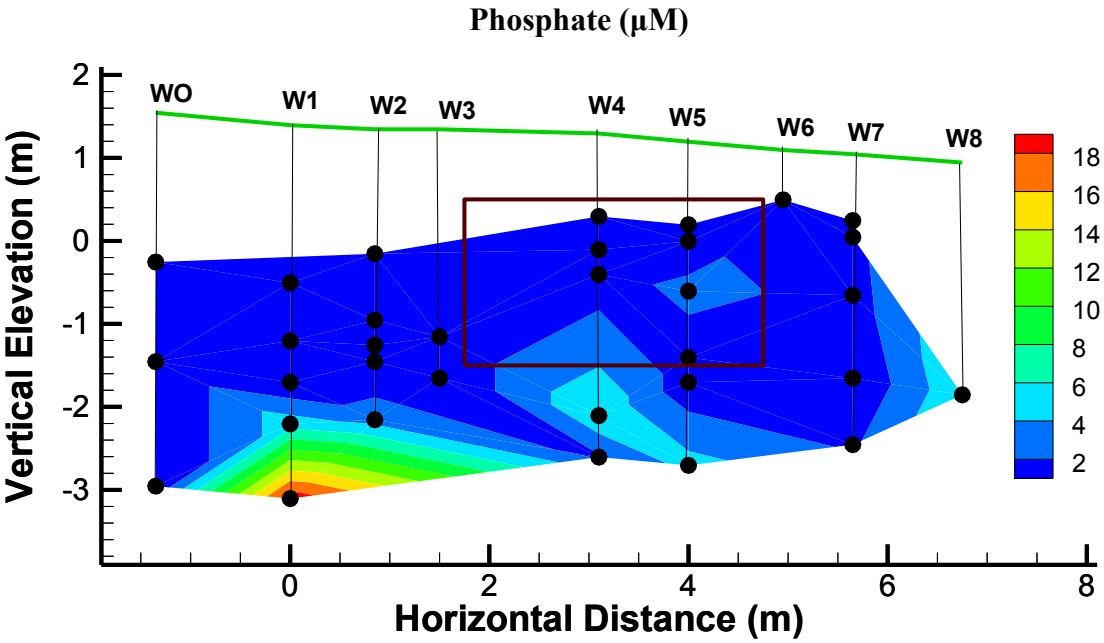

Appendix 3. Cl^- concentrations (mM) versus salinity in sampling wells inside, up-gradient, down-gradient and underneath the PRB.

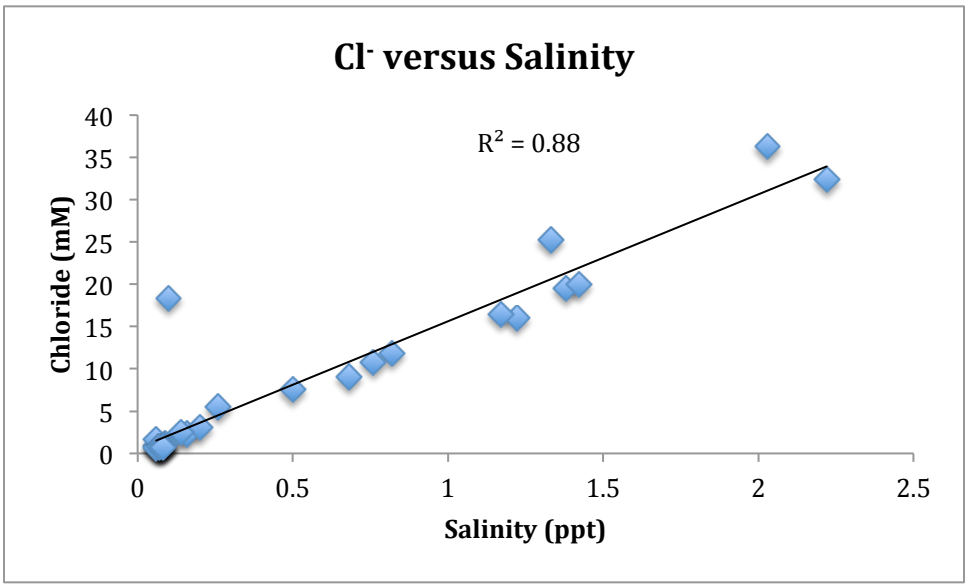

Appendix 4. Copy number/ng DNA of the nirS gene from qPCR in sampling wells. Samples 1-4 are up-gradient of the PRB in well 0, well 1 and well 3; Samples 5 and 6 are in the PRB in well 5; Sample 7 is just underneath the PRB in well 5; sample 8 is far underneath the PRB in well 5; and samples 9-12 are in well 7 down-gradient of the PRB.